Busbar Current Transducer With Suppression of External Fields and Gradients

Pavel Ripka and Andrey Chirtsov

Faculty of Electrical Engineering, Czech Technical University in Prague, 16627 Prague, Czech Republic.

Yokeless busbar current transducers with circular sensor array achieve high precision when replacing Hall sensors by microfluxgate. Limited field range of fluxgate can be compensated by inverse design with sensors inside the busbar. In this paper, we present a novel scheme how to improve the immunity of such sensor against external field and field gradient. We also examine crosstalk error for external currents close to the transducer. Using five microfluxgate sensors, we designed a 400 A current transducer which has a suppression of 93 000 for currents in 40 cm vicinity.

Index Terms— **Current transducer, fluxgate.**

I. Introduction

YOKELESS busbar current sensors are cheap and compact, but they are sensitive to external magnetic fields and field gradients [1], [2]. We have described a current transducer based on a couple of microfluxgate sensors [3] inside the cylindrical hole in the busbar [4], [5]. The advantage of this transducer is high range and small size compared with similar transducers based on a circular sensor array around the conductor [6]. Compared with Hall current sensors [7], [8], a fluxgate current sensor has 10 times better stability. Solution based on anisotropic magnetoresistors (AMR) has 10 times lower range due to the small saturation field of AMR sensors [9].

Using only two sensors in differential mode gives only small immunity against crosstalk: in [2], we have shown that lateral current in 15 cm vicinity is suppressed only by the factor of 66. In [10], we have suggested that better suppression of the magnetic fields generated by external currents can be achieved by using four microfluxgate sensors: two of them are active and they measure y-component of the field at points A and C (B_{Ay} and B_{Cy}) and the other two measure both field components at point B (B_{Bx} and B_{By}). Unfortunately, this approach can be effective only for the case of known geometry of the external currents or when the external currents are also measured.

However, in general case, the position and size of the external current is not always known and the interference field can be generated by several currents simultaneously. Significant magnetic fields can also be generated by coils and by magnetic materials (both hard and soft in external field) in the vicinity of the transducer.

In this paper, we therefore suggest more general approach and we show the design of current transducer which is immune to external homogeneous fields and first-order field gradients. This means that our new solution does not perfectly compensate the field from external conductors, but effectively suppresses their influence, as higher order gradients from distant currents are small.

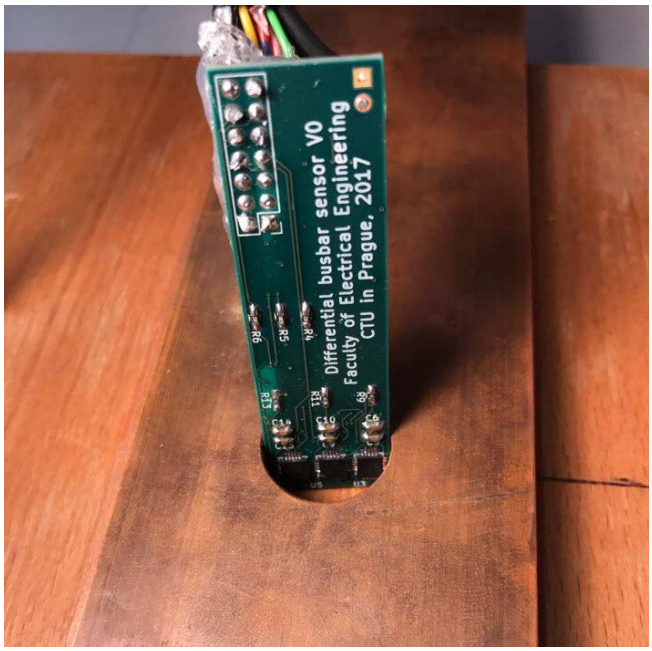

Fig. 1. Current busbar with a fluxgate sensor array inserted into the hole.

We start from 2-D FEM simulation and find points, which can be used to compensate the influence of the external fields and field gradients. Using the field values at these points, we derive the formula for the measured current. Finally, we verify the design by measurement.

II. Transducer Design

Fig. 1 shows the current busbar with a fluxgate scanning sensor array inserted into the hole and Fig. 2 shows field distribution on a busbar cross section. The size of the copper busbar is 6 cm × 1 cm and the hole diameter is 19 mm. The dc current value for this simulation was 1000 A. The sensor array shown in Fig. 1 consists of six sensors: three of them are visible as a row with 6 mm pitch, which measures B_y in positions A, B, and C. The other three sensors are on the opposite side of the printed circuit board and they measure B_x at the same points. By moving this sensor array in y-direction,

Manuscript received March 16, 2018; revised May 1, 2018; accepted May 30, 2018. Date of publication June 22, 2018; date of current version October 17, 2018. Corresponding author: P. Ripka (e-mail: ripka@fel.cvut.cz).

Color versions of one or more of the figures in this paper are available online at http://ieeexplore.ieee.org.

Digital Object Identifier 10.1109/TMAG.2018.2844254

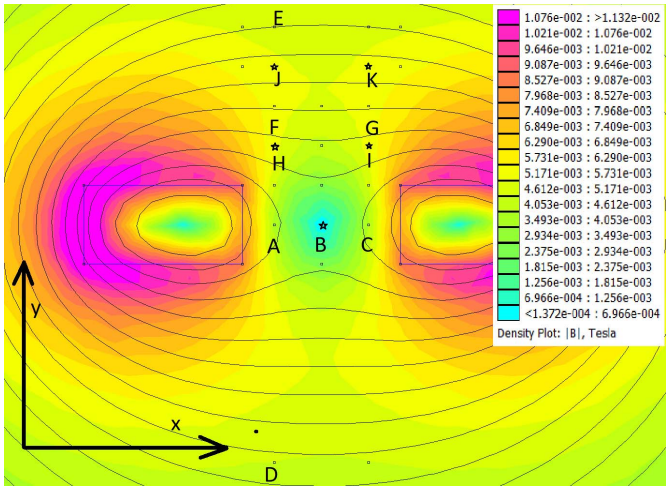

Fig. 2. Field distribution shown on a cross section. The dc current value for this simulation was 1000 A. Final position of the sensors selected for the current transducer is marked by stars.

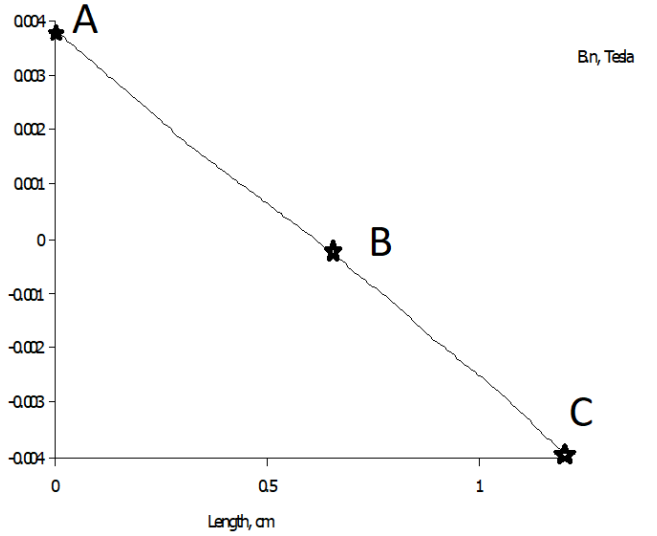

Fig. 3. B_y field profile from the measured 1000 A current calculated along the A-C line. Points A, B, and C correspond to points in Fig. 2. The stars show position of the sensors according to Fig. 2.

we can scan the field values at other positions above the central plane and verify the simulations. In general, the fit between our measurements and FEM simulations is within 5%. After performing the simulation and measurement exercise, we fixed the sensor optimum position for the final transducer design, which is shown in Figs. 6 and 7.

All previously published current transducers of this type such as [3] and [7] used sensors in the central line (positions A and C) for measuring B_y. The fact that B_{Ay} and B_{Cy} have opposite sign was used to suppress homogeneous external field B_0. However, calculated field distribution of B_y along the A-C line is linear (Fig. 3) and this means that external dB_y/dx field gradient cannot be suppressed. Possible solution of this problem would be to change the busbar geometry in order to achieve significantly non-linear field profile and evaluate the second-order gradient from the measured current. We have made extensive simulations with

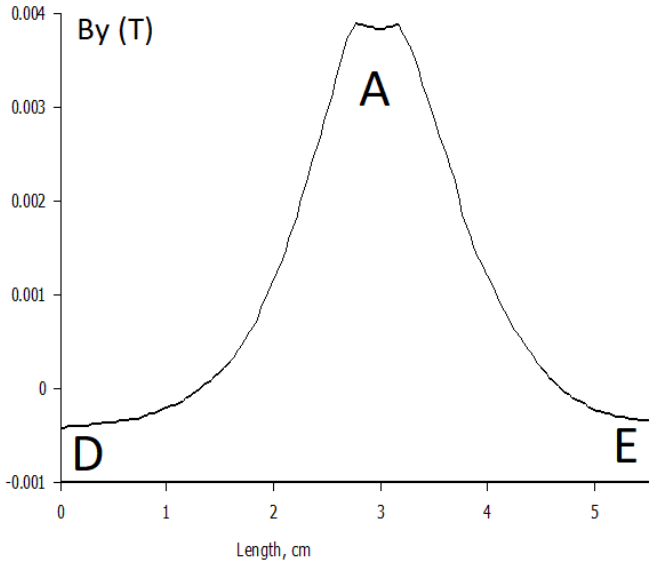

Fig. 4. B_y field profile calculated across the D-E line.

various geometries, but we never achieved significant non-linearity. Instead of that, we decided to find alternative sensor positions outside the central A-C line. Fig. 4 which shows B_y field calculated along the D-E line. The field profile in the vicinity of central point A is flat which indicates good sensor stability against small sensor displacement caused by manufacturing tolerances and temperature dilatations. On the profile, we can also find positions, where the field from the busbar current is zero. These points could be theoretically used to locate compensation sensors to suppress field gradients. However, the sensitivity in these points is steeply changing, which makes them susceptible to the mentioned displacements.

The novelty of our approach is that we use B_x instead of B_y. B_x response to the measured current does not change sign when mirroring around the y-axis. At H and I points, the calculated sensitivity is the same, 5 mT/1000 A as shown in Fig. 5. Due to the 2 mT maximum range of the DRV425 sensor, the actual current range will be only 400 A. Summing $B_{Hx} + B_{Ix}$, therefore, does not suppress homogeneous external field B_{0x}, but instead of that it suppresses dB_x/dx field gradient. This type of gradient is not typical for long conductors, but is typical for dipolar sources such as coils and permanent magnets. This setup is also completely insensitive to the external currents in y (superior)-direction. The dependence on B_{0x} can be suppressed by using the third x-sensor at the central point A. Remaining is the dependence on dB_x/dy field gradient. Here, we face the similar problem as before, because B_x response to the measured current change sign when mirroring around the x-axis. Fortunately, the calculated field distribution along the D-E line is strongly non-linear, and thus, the external dB_x/dy field gradient can be suppressed. This is documented by the B_x profile calculated along the D-E line (Fig. 5). We achieve the required compensation by using additional sensor located at J and eventually also K point. While $B_{Jy}-B_{hy}$ is insensitive to the measured current, this value depends only on dB_y/dx field gradient.

The schematics of our novel transducer design are shown in Fig. 6: it consists of five sensors: B, H, I, J, and K. The

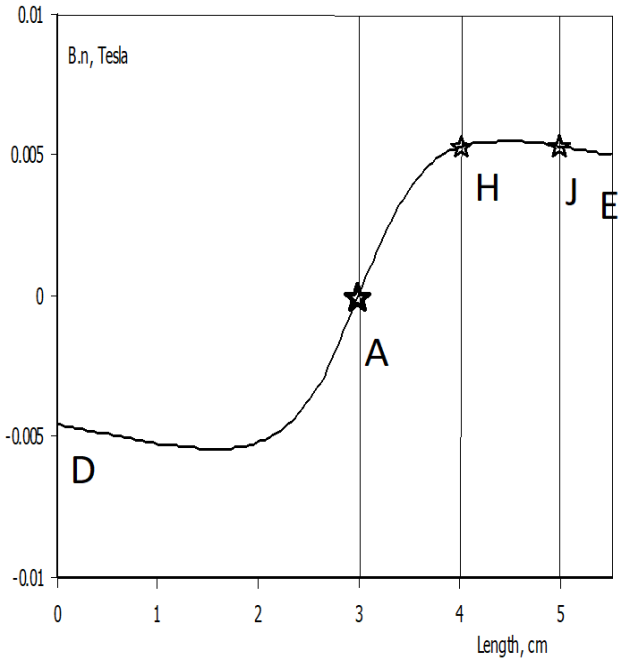

Fig. 5. B_x field calculated along the D-E line. The stars show position of the sensors according to Fig. 2.

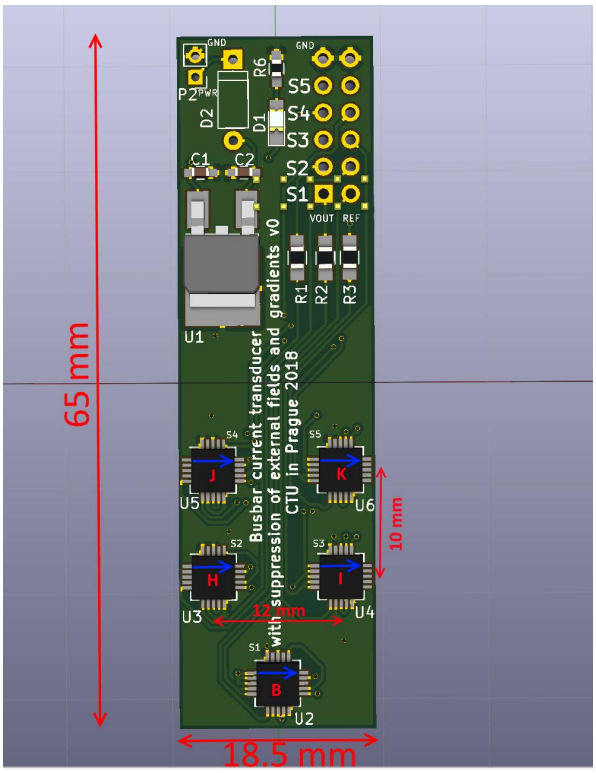

Fig. 6. Schematics of our new transducer. Sensors are labeled B, H, I, J, and K, as shown in Fig. 2.

sensor position corresponds to stars in Fig. 2. Fig. 7 shows the final sensor board inserted into the busbar.

A. Finding the Compensation Formula

Let us assume that the external field at point B equals to B_0 and the external field gradient $dB/dx = B_1/6$ mm and $dB/dy = B_2/10$ mm. And let us denote B_m as the field from the measured current.

Fig. 7. Photograph of the new transducer in the working position. The sensor B (at the bottom) is located in the center of the busbar.

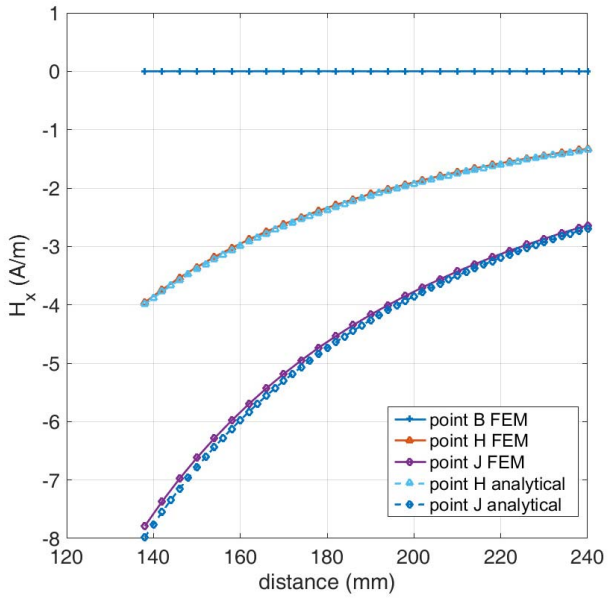

Fig. 8. Response to lateral current—simulation and analytical.

Then, we can write

$$B_B = B_0 \tag{1}$$
$$B_H = B_0 - B_1 + B_2 + B_m \tag{2}$$
$$B_I = B_0 + B_1 + B_2 + B_m \tag{3}$$
$$B_J = B_0 - B_1 + 2B_2 + B_m \tag{4}$$
$$B_K = B_0 + B_1 + 2B_2 + B_m \tag{5}$$
$$B_H + B_I - 2B_B = 2B_2 + 2B_m \tag{6}$$
$$B_J + B_K - 2B_B = 4B_2 + 2B_m \tag{7}$$
$$B_J + B_K - 2B_B - 2B_H - 2B_I + 4B_B = -2B_m \tag{8}$$
$$B_m = B_H + B_I - (B_J + B_K)/2 - B_B \tag{9}$$

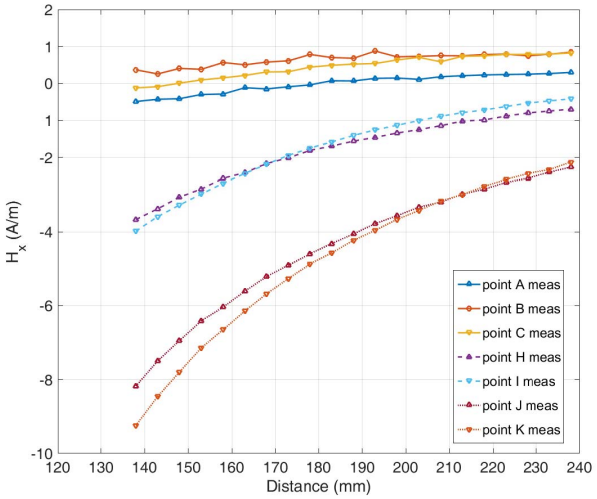

Fig. 9. Response to lateral current—measurement.

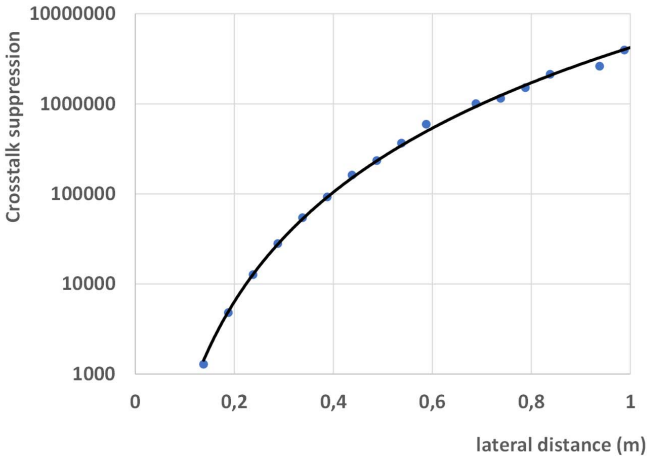

Fig. 10. Crosstalk suppression for lateral external current as a function of its distance. The measured values are shown as data points, and the line is polynomial trend and serves only as a guide to the eye.

Finally, the formula for the measured field B_m is

$$B_m = B_H + B_I - (B_J + B_K)/2 - B_B \tag{10}$$

From this formula, the resulting sensitivity for B_m is still 5 μT/A. As the noise of individual sensors is not correlated, the fluxgate sensor noise is suppressed by $\sqrt{4}$.

III. Verification

Fig. 8 shows field caused by the external current in the location of all sensors. The field is calculated by two methods: analytically, supposing that the external current flows through the idealized single line conductor, and by FEM taking into account the real size of the 60 mm × 10 mm current bar. It is clear that for distances larger than 20 mm, the size of the external conductor does not influence the results.

Fig. 9 shows the same values measured by uncalibrated sensors. The differences from ideal results shown in Fig. 6 were analyzed, and it was shown that error is caused more by sensor rotation than by displacements.

If we use formula (10), external homogeneous fields and first-order field gradients are compensated. Fig. 10 shows how effectively the lateral current is suppressed. The measured suppression increases fast with the distance: while in the distance of 14 cm it is 1300, it is already 93 000 in the 40 cm distance and 4 million in the distance of 1 m. The superior current is suppressed ideally as its contribution to $B_H = B_I$ and also $B_J = B_K$.

IV. Conclusion

By using a novel geometry of the fluxgate current transducer, we achieve compensation of external fields and first-order field gradients. External superior currents are suppressed completely, while the worst influence have the lateral currents which are suppressed by the factor of 1300 in the 14 cm distance, which is significantly more than the suppression of 66 achieved in the same distance with differential transducer using two fluxgates [2]. The only disadvantage of the proposed solution is that transducer full-scale range was reduced from 1000 to 400 A.

Acknowledgment

This work was supported by the Grant Agency of the Czech Republic through the Project New Methods for the Measurement of Electric Currents under Grant GACR 17-19877S. The work of A. Chirtsov was supported by Texas Instruments.

References

[1] P. Ripka, "Electric current sensors: A review," *Meas. Sci. Technol.*, vol. 21, no. 11, pp. 112001-1–112001-23, 2010.
[2] P. Ripka and A. Chirtsov, "Influence of external current on yokeless electric current transducers," *IEEE Trans. Magn.*, vol. 53, no. 11, Nov. 2017, Art. no. 4003904.
[3] M. F. Snoeij, V. Schaffer, S. Udayashankar, and M. V. Ivanov, "Integrated fluxgate magnetometer for use in isolated current sensing," *IEEE J. Solid-State Circuits*, vol. 51, no. 7, pp. 1684–1694, 2016.
[4] D. W. Lee *et al.*, "Fabrication and performance of integrated fluxgate for current sensing applications," *IEEE Trans. Magn.*, vol. 53, no. 11, Nov. 2017, Art. no. 4004204.
[5] P. Ripka, V. Grim, and V. Petrucha, "A busbar current sensor with frequency compensation," *IEEE Trans. Magn.*, vol. 53, no. 4, Apr. 2017, Art. no. 4000505.
[6] R. Weiss, R. Makuch, A. Itzke, and R. Weigel, "Crosstalk in circular arrays of magnetic sensors for current measurement," *IEEE Trans. Ind. Electron.*, vol. 64, no. 6, pp. 4903–4909, Jun. 2017.
[7] K.-L. Chen and N. Chen, "A new method for power current measurement using a coreless Hall effect current transformer," *IEEE Trans. Instrum. Meas.*, vol. 60, no. 1, pp. 158–169, Jan. 2011.
[8] M. Blagojević, U. Jovanović, I. Jovanović, D. Mančić, and R. S. Popović, "Realization and optimization of bus bar current transducers based on Hall effect sensors," *Meas. Sci. Technol.*, vol. 27, no. 6, 2016, Art. no. 065102.
[9] P. Mlejnek and P. Ripka, "Off-center error correction of AMR yokeless current transducer," *J. Sensors*, vol. 2017, Oct. 2017, Art. no. 6057634.
[10] P. Ripka, "4-sensor yokeless electric current transducer," in *Proc. IEEE Int. Magn. Conf. (INTERMAG)*, Dublin, Ireland, Apr. 2017, p. 1.